Spin physics with light and heavy neutral mesons at Protvino

V. V. Mochalov, S. V. Ivanov, V. I. Garkusha, A. S. Gurevich,
V. I. Kravtsov, O. P. Lebedev, N. I. Minaev, L. V. Nogach,
S. B. Nurushev, A. N. Vasiliev

IHEP, Protvino, Russia

A. V. Otboev, Yu. M. Shatunov, D. K. Toporkov

BINP, Novosibirsk, Russia

A. S. Belov

INR, Moscow, Russia

PROZA-M experiment results as well the proposal of a new spin program with the use of a polarized proton beam are presented. Significant asymmetries were observed in inclusive π^0 production. The new program proposes to study a wealth of single- and double-spin observables in various reactions using longitudinally and transversely polarized proton beams at U70. The main goal is to define gluon contribution to nucleon spin by measuring double-spin asymmetry in charmonium production.

PACS: 13.20.Cz, 13.20.Fc, 13.20.Gd, 13.88+e

Key words: Nucleon spin, polarization, transversity, single-spin asymmetry, double-spin asymmetry, charm production

1 Introduction

Polarization experiments give us an unique opportunity to probe the nucleon internal structure. While spin averaged cross-sections can be calculated within acceptable accuracy, current theory of strong interactions can not describe large single-spin asymmetries and polarization. Unexpected large values of single spin asymmetry (SSA) in inclusive π-meson production are real challenge to current theory because naive perturbative Quantum Chromodynamics (QCD) predicts small asymmetries due to the helicity conservation decreasing with transverse momentum increase.

Although years of experimental efforts at miscellaneous accelerators have provided a lot of information about the QCD hard scattering and the parton structure of the proton, there is no corresponding body of data on the spin-dependence of the elementary interactions and the spin structure of the proton. High intensity polarized proton beam to be accelerated up to 70 GeV and extracted from U70 main ring would offer the opportunity to study the unique properties of the spin variable at large x to increase the understanding of these fundamental quantities.

We present the result of SSA measurements at PROZA experimental setup (section 2) as well as the proposal of new experiments with polarized proton beam at 70 GeV proton synchrotron of IHEP-Protvino (section 3).

2 Single-spin asymmetry in inclusive π^0 production.

The PROZA collaboration started to study SSA measurements of neutral mesons 30 years ago. Comprehensive study of exclusive charge-exchange reactions pointed out to significant spin effects [1]. To investigate the dependence of the asymmetry on beam particle flavor and energy as well as on secondary meson production angle, the measurements were carried out at the central and polarized target fragmentation region at the energy range 40–70 GeV in the reactions:

$$\pi^- + p_\uparrow(d_\uparrow) \to \pi^0(\eta) + X \tag{1}$$

$$p + p_\uparrow \to \pi^0 + X \tag{2}$$

Single spin asymmetry A_N is defined as

$$A_N(x_F, p_T) = \frac{1}{P_{\text{targ}}} \cdot \frac{1}{\langle\cos\phi\rangle} \cdot \frac{\sigma_\uparrow^H(x_F, p_T) - \sigma_\downarrow^H(x_F, p_T)}{\sigma_\uparrow^H(x_F, p_T) + \sigma_\downarrow^H(x_F, p_T)} \tag{3}$$

where P_{targ} is the target polarization, ϕ is the azimuthal angle between the target-polarization vector and the normal to the plane spanned by the beam axis and the momentum of the outgoing neutral pion, and $d\sigma_\uparrow^H$ ($d\sigma_\downarrow^H$) are the invariant differential cross sections for neutral-pion production on hydrogen for opposite directions of the target-polarization vector. We detected neutral pions in the azimuthal angle range of $180 \pm 15\,°$; therefore, we set $\cos\phi = -1$. Since the π^0's detection efficiency is identical for the two directions of the target polarization vector, we find for the detector on the right side of the beam, that

$$A_N = -\frac{D}{P_{\text{targ}}} \cdot A_N^{\text{raw}} = -\frac{D}{P_{\text{target}}} \cdot \frac{n_\uparrow - n_\downarrow}{n_\uparrow + n_\downarrow} \tag{4}$$

where A_N^{raw} is the raw asymmetry actually measured in the experiment, D is the target-dilution factor, and $n_\uparrow$ ($n_\downarrow$) are the normalized (to the monitor) numbers of detected neutral pions for up and down directions of the target-polarization vector. The procedure used to calculate D was described in detail elsewhere [2].
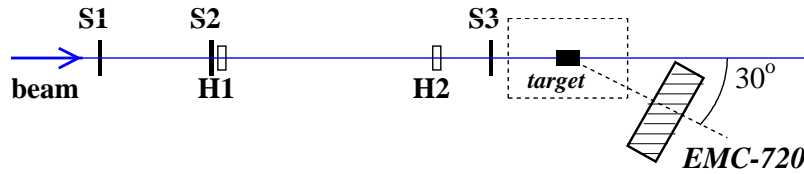

Fig. 1. Experimental Setup PROZA-M. S1-S3 – trigger scintillation counters; H1–H2 — hodoscopes; $EMC1$–$EMC3$ — electromagnetic calorimeters; *target* — polarized target.

Current configuration of the PROZA-M Experimental Setup [3] is presented on **Fig. 1**. The beam of negatively charged particles produced in the internal target was deflected into the beam-line by guide magnetic field of the accelerator. For the first time the proton beam was extracted from a strong-focusing synchrotron U70 by the thin **Si** crystal bent under 80 mrad [4, 5]. A frozen propane-diol ($C_3H_8O_2$) target with an average polarization 85 % was used [6]. Beam particles were detected by the two two-coordinate hodoscopes H1–H2, placed 8.7 and 3.2 m downstream the target. Three scintillation counters S1–S3 were used for a zero level trigger. γ-quanta were detected by the total absorption electromagnetic calorimeters *EMC* (array of 720 lead-glass cells [7]). The counters were of size $38 \times 38 \times 450$ mm^3 (18 rad. length). Currently the detector is situated 2.3 m downstream the target at 30 ° at laboratory frame to measure the asymmetry in the polarized target fragmentation region.
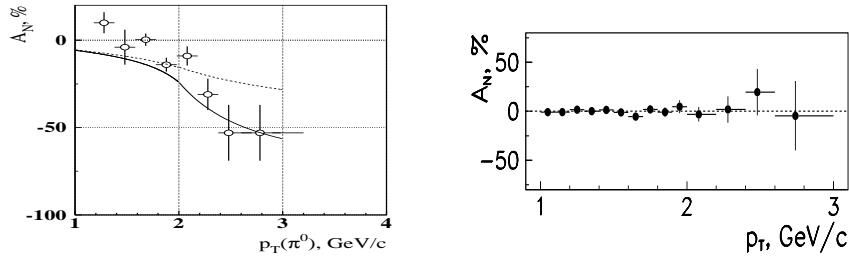

Fig. 2. Left: summary A_N for the reaction $\pi^- + p_\uparrow(d_\uparrow) \to \pi^0(\eta) + X$; right: A_N for the reaction $p + p_\uparrow \to \pi^0 + X$; both at the central region. Solid line — predictions for U-matrix model [10], dashed — for the model with quark chromomagnetic moment [11].

A_N in the central region was measured for the reactions $\pi^- + p_\uparrow(d_\uparrow) \to \pi^0(\eta) + X$ [2, 8] and in the reaction $p + p_\uparrow \to \pi^0 + X$ [9] in wide range of transverse momenta (**Fig. 2**). Asymmetry is consistent with zero in *pp*-interaction, while significant effect was observed in the reaction (1). One may conclude that the asymmetry in the central region depends on quark flavor.
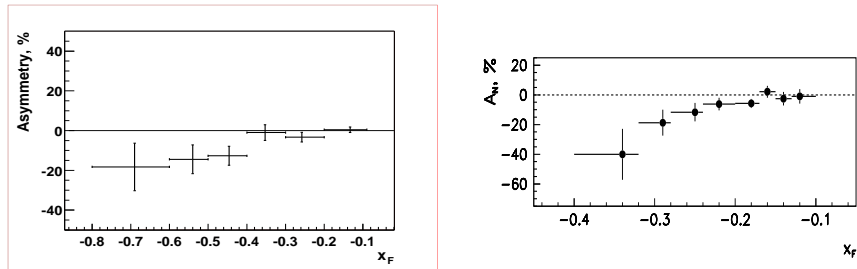

Fig. 3. A_N in the reaction $\pi^- + p_\uparrow \to \pi^0 + X$ at 40 GeV (left) and in the reaction $p + p_\uparrow \to \pi^0 + X$ at 70 GeV (right) in the polarized target fragmentation region.

SSA in the target fragmentation region (see **Fig. 3**) was measured in the reaction $p + p_\uparrow \rightarrow \pi^0 + X$ at 70 GeV [12] and in the reaction $\pi^- + p_\uparrow \rightarrow \pi^0 + X$ at 40 GeV [13]. Asymmetry is consistent with zero at small absolute values of scaling variable x_F, then starts to grow up in the magnitude and achieves significant values. The asymmetry does not depend on beam particle flavor in the polarized target fragmentation region.

Universal threshold of single-spin asymmetry in inclusive pion production was found for fixed target experiments [14]. The asymmetry is consistent with zero below threshold energy value in the center of mass system and then starts to grow up. The result of the threshold energy for different experiments is presented in **Fig. 4**. The effect may points out the existence of complex structure inside constituent quark [15].

We continue to study asymmetry in the reaction $p + p_\uparrow \rightarrow \pi^0 + X$ at intermediate and large negative values of x_F. During first stage of the measurements we have accumulated enough statistics to achieve accuracy in pp-interaction at intermediate negative values of x_F at the same or even better level as for $\pi^- p$-interactions. The expected accuracy will allow us to check "universal threshold" . The statistics in the reaction(2) will be increased at least by factor of four during 2007 data-taking run, especially for large negative values of x_F.

Nevertheless to investigate universal threshold for different particles and in different kinematic regions polarized proton beam is required.
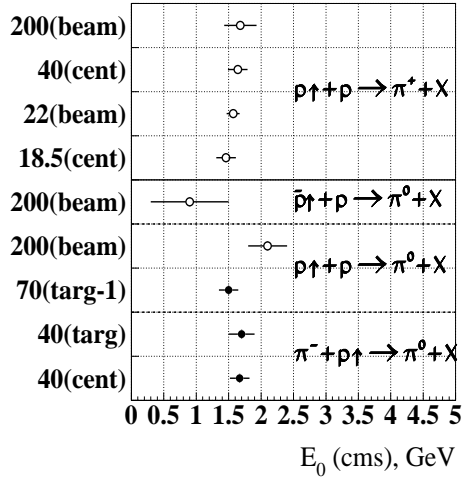
Fig. 4. Center of mass energy values where the pion asymmetry starts to grow up for different experiments. The energy along the Y-axis is in GeV; *cent* — corresponds to experiments in the central region ($x_f \approx 0$), *targ* — the polarized target fragmentation region; *beam* – the polarized beam fragmentation region.

3 Experiments with polarized proton beam at U-70

New program of spin experiments is developing now at IHEP. We propose to produce a polarized proton beam from the polarized atomic beam-type source, accelerate it up to 70 GeV and deliver to several experimental setups to:
  − measure the gluon and quark polarization in longitudinally polarized protons in charmonium production;
  − study transversity distribution by measuring the double-spin asymmetry for the Drell–Yan muon pair production;
  − measure the dependence of single-spin asymmetries on separate kinematic variables p_T and x_F and hadron flavor to study the it's origin;

– measure miscellaneous spin parameters in hyperon production at moderate transverse momenta to learn about the role of strange quarks in the spin structure of nucleon;
– measure polarization and spin correlation parameters in elastic pp-scattering in the hard scattering region in order to check the QCD predictions.

Final goals of spin physics at U70 are :
– study the spin structure of the proton, i.e., how the proton's spin state can be obtained from a superposition of Fock states with different numbers of constituents with nonzero spin;
– study how the dynamics of constituent interactions depends on spin degrees of freedom and on the flavors;
– understand chiral symmetry breaking and helicity non-conservation on the quark and hadron levels;
– study the overall nucleon spin structure in the range of moderate p_T (up to 5 GeV/c), and the long range QCD dynamics (confinement), including study non-perturbative interactions of massive constituent quarks with an effective color field of flux tubes, produced by confined quarks and gluons.

These issues are closely interrelated at the hadron level and the results of the experimental measurements are to be interpreted in terms of hadron spin structure convoluted with the constituent interaction dynamics.

3.1 Acceleration of polarized proton beam

To do this spin physics, the polarized proton beam with an intensity up to $5 \cdot 10^{12}$ protons per spill and energy up to 70 GeV needs to be accelerated. This process requires the development of intensive polarized proton source, acceleration of the polarized beam in 1.5 GeV booster and U-70 main ring, extraction of the beam onto experimental setup. Development of beam polarimetry and polarized targets is also required

3.1.1 Polarized Ion Source

To reach an intensity of the polarized proton beam in the U-70 accelerator higher than 5×10^{12} p/cycle one needs to design and build a high intensity source. The technique of sources with optical pumping (optical) or with resonant charge-exchange plasma ionizer (atomic) has been successfully developed for last decades. The following characteristics of the existing and developing sources are presented in **Table. 1**: type of the source, peak intensity I, polarization P, emittance, pulse duration, repetition rate, figure of Merit $P^2 \cdot I$ and modified figure of merit $P^2 \cdot I \cdot N$ [1]).

A high intensity pulsed source of polarized protons and negative polarized hydrogen ions built at the Institute of Nuclear Research (INR) in Troitsk [16] have

---

[1]) N is number of turns of polarized ion beam during its stripping injection into the booster ring.

the record figure of merit $P^2 \cdot I$. The polarized ions are being generated as a result of the charge exchange reaction between the polarized hydrogen atoms and the unpolarized deuterium ions in the deuterium plasma. This source gives polarized protons of 11 mA in the pulsed mode with polarization $P = 80\%$. For the negative polarized hydrogen atoms the pulsed current I is 3.8 mA and the polarization is 90 %. The similar source produced at IUCF in collaboration with INR was successfully used at the Indiana University in USA. The source operation demonstrated a long term stability and reliability. The source current can be increased further by using of sextupole separating magnets with magnetic field up to 5 T.

Table 1. Characteristics of different polarized ion sources

Lab.	Type	I, (mA)	P	Emitt. (mm·mrad)	Pulse duration (msec)	Rep., rate (Hz)	$P^2 \cdot I$	$P^2 \cdot I \cdot N$
RHIC (BNL)	Optical $H_\uparrow^-$	1	0.82	2π	0.5	1	0.67	14.7
TRIUMF /INR	Optical $H_\uparrow^-$	8	0.42	2π	0.1	1	1.4	30.8
	$H_\uparrow^+$	50	0.5	2π	0.1	1	12.5	12.5
INR, Moscow	Atomic $H_\uparrow^-$	3.8	0.91	1.7π	0.17	5	3.15	69.3
	$H_\uparrow^+$	11	0.8	1.0π	0.2	5	7.0	7.0
IUCF	Atomic $H_\uparrow^-$	1.6	0.85	1.2π	0.3	2	1.2	26.4
	$D_\uparrow^-$	1.8	0.9	1.2π	0.3	2	1.2	26.4
COSY	Atomic $H_\uparrow^-$	0.02	0.9	0.5π	10	0.5	0.016	0.35
	$D_\uparrow^-$	0.02	0.9	0.5π	10	0.5	0.016	0.35
JINR	Atomic $D_\uparrow^+$	0.4	0.6		0.4	0.1	0.144	0.144

3.1.2 Conservation of the polarization during acceleration

During acceleration, the polarization may be lost when the spin precession frequency passes through a so-called depolarizing resonance. These resonances occur when the spin tune $\nu_{sp} = \gamma \times G$ (where $G = 1.793$ is the anomalous magnetic moment of the proton and $\gamma = E/m$) is equal to an integer number (imperfection resonances), or equal to $kP \pm \nu_z$ (intrinsic resonances). Here $P = 12$ is the superperiodicity of the U70 accelerator (or its booster), ν_z is the vertical betatron tune, and k is an integer. Imperfection resonances are due to vertical closed orbit errors and intrinsic resonances are due to the vertical betatron motion.

There are four strong resonances in 1.5 GeV booster (**Table. 2**). There is no space inside booster for pulsed quads to pass resonances using fast jump of the betatron frequency. Nevertheless the polarization in booster is still expected to be conserved at the level of 70 % even without any modification of the booster. We study three possible ways to decrease depolarization inside booster:

– to inject the beam to main ring at the energy close to 1 GeV. In this case last two resonances are obsolete and the depolarization in booster will be 15 %

– the strength of imperfection resonances can be decreased by proper vertical orbit correction and decreasing of the beam emittance.

– the strength of last two resonances may be increased to flip spin direction by some blow-up of beam emittance.

Table 2. Strong resonances at booster

Resonance ν_z	$\nu_{\rm sp}$	$W_{\rm kinet}$	P_f/P_i
2	2	0,108	0,96
3	3	0,631	0,89
4	4	1,155	$-0,89$
$0 + Q_Z$	3,78	1,040	$-0,93$

3.1.3 Polarization at main ring

The number of resonances at U-70 and their strength (**Fig. 5**) is too large to overcome them without inserting into machine lattice a special array of magnets, which will rotate spin (syberian snakes) [17]. There are a number of schemes with combinations of solenoids and skew quads, that don't cause the coupling out side the insertion. But such schemes require, as a rule, a long straight section. Compact partial snakes can be designed of helical magnets [18]. Spin rotations by transverse fields don't depend on energy for high energy particles whereas the action on spin by longitudinal fields is inversely proportional to the energy. Orbit distortions due to transverse fields can be minimized in the case of helical magnets by a dedicated snake design comprising a set of four full twist helixes with mirror symmetry and
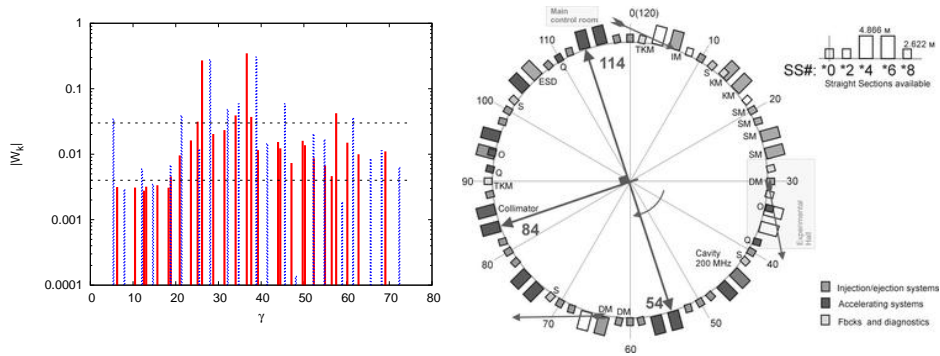

Fig. 5. Resonances at U-70 main ring:
solid — imperfection, dashed — intrinsic. Fig. 6. Snake position proposed for the U-70.

adjusted field levels. A partial snake rotates spin only by a few degrees. First beam test of this concept have been done in 1976 year at electron-positron collider VEPP-2M [19]. Later the solenoidal partial snake was applied at AGS, where polarized protons are accelerated up to 25 GeV.
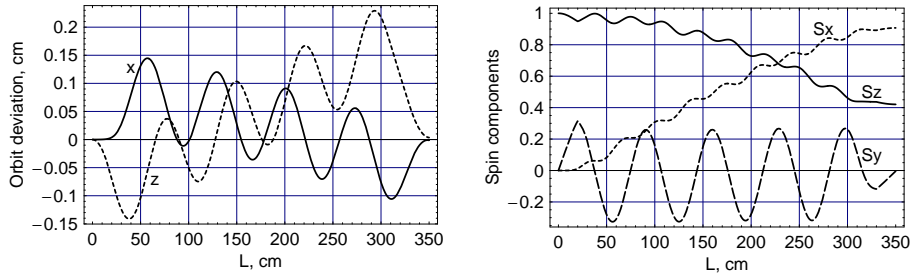

Fig. 7. Closed orbit distorsion (left) and spin rotation (right) inside the snake

The present proposal suggests installing three identical partial snakes into three super-periods of U-70, as it's shown in **Fig. 6**. Each snake occupies 3.5 m longitudinally and consists of a 4-period helix ($\lambda = 70$ cm; aperture 15 cm) with field up to 4.2 T. This combination rotates spin by 65°. To compensate for some optics distortion ($< 5\%$) two dipole coils are wounded at the edges.

Particle trajectories inside the snake and spin rotation by the snake per pass are shown in **Fig. 7** for the beam energy 25 GeV. The spin rotations by all the snakes with identical polarities are added coherently at $\nu_0 = k = m \cdot P/4$ (m are integers) or at $\nu_0 = k = (m + 1/2) \cdot P/4$ with one snake polarity being reversed. The last option looks more suitable for U-70.

Proposed schemes using three helical partial snakes at U-70 can provide acceleration of polarized protons up to top energy E = 70 GeV under conditions of conservation of normalized vertical emittance accepted from the booster through a whole acceleration cycle and alignment requirements for machine magnets of around ± 0.5 mm. Spin tracking study proves the possibility to preserve polarization at a
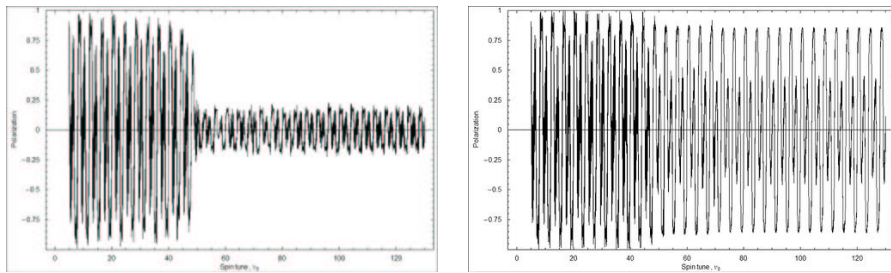

Fig. 8. Spin tracking of vertical polarization for 30 particles with two values of betatron tunes $\beta_Z = 9.70$ (left) and $\beta_Z = 9.94$ (right)

high level while setting the prescribed vertical betatron tune $\beta_Z = 9.94$ (**Fig. 8,** right) in course crossing the spin resonance.

3.1.4 Extraction of polarized proton beam

The beam depolarization during extraction seems to be neglectable because transversely (vertical) polarized beam is deflected in horizontal direction by vertical field. Stochastic method of beam slow extraction (being developed at IHEP) is seems applicable for polarization conservation to extract the particles from the beam core. Expected values of relative polarization (in respect to polarization in main ring) as well as beam characteristics are presented in **Table 3**. Depolarization in the beam transfer line magnet elements is also very small due to:

– Relatively small $p^\uparrow$ beam emittance (if to compare with secondary beams);
– Opposite direction of magnetic field in focusing and defocusing lenses.

Table 3. Extracted Beam characteristics at the experimental setups

Experimental setup	SVD	SPIN	FODS	SPASCHARM
Size in horiz. plane, (σ_x, mm)	1.09	0.58	1.57	0.22
Size in vert. plane, (σ_y, mm)	0.84	0.94	1.42	1.56
Beam polarization, (s_y)	0.96	≈ 1	0.99	≈ 1

3.1.5 Polarimetry

There should be two types of polarimeters at U70:

1. absolute polarimeter to determine a value and a sign of polarization with a high accuracy and
2. less accurate but fast relative polarimeter.

The both polarimeters should be based on Coulomb-Nuclear Interference (CNI) effect. The absolute polarimeter could be built with the use of a polarized jet target, while the relative polarimeter with the use of Carbon thin target. The absolute polarimeter is requred to calibrate the relative one. The absolute value of the beam polarization in the U70 averaged over 50 hours data taking could be measured to 5 % statistical accuracy with the use of polarized hydrogen jet. Relative polarimeter allowes to measure beam polarization with the same accuracy 5 % each two minutes.

3.2 Proposal of the experiment SPASCHARM

The study of spin effects in some processes would yield information on the contribution of the spin of quarks $\Delta\Sigma$ and gluons ΔG and orbital angular momenta of quarks L_q and gluons L_g into the hadron helicity:

$$1/2 = 1/2\Delta\Sigma + L_q + \Delta G + L_g \tag{5}$$

In the above sum all terms have clear physical interpretation, however besides the first one, they are gauge and frame dependent. At present only 1/3 of the longitudinally polarized proton spin is described by quark's spin. 70 % of proton spin may be explained by gluon and/or orbital moment contributions. Experiments at CERN, HERA, SLAC (polarized lepton beams) measured mainly quark polarization for last 15 years. COMPASS and HERMES are trying to measure gluon polarization at small $x = 0, 1$–0.15. RHIC experiments (A_{LL} in direct gamma production) begin to measure gluon polarization at very low values of x (≈ 0.01) whereas gluon polarization should be measured in a whole range of x.

We propose to simultaneously measure the double-SPin ASymmetry A_{LL} in CHARM production (SPASCHARM) for inclusive χ_2, χ_1 and J/ψ by utilizing the $70\,\mathrm{GeV/c}$ longitudinally polarized-proton beam on a longitudinally polarized target. Our goal is to obtain besides the quark-spin information also the gluon-spin information from these three processes in order to determine what portion of the proton spin is carried by gluons. One of the possible ways to measure such parton's polarization is a study of χ_c-meson production with the following decay into J/ψ and a photon and then $J/\psi \to \ell^+\ell^-$. It was shown in [20], that the angular distribution of the final photon and lepton pairs provides a direct way to measure the polarization of the initial quarks and gluons. We anticipate obtaining significant numbers of χ_2, χ_1 and J/ψ events. This would be the world's first measurement of gluon-spin information and of spin effects in charmed-particle production in hadron-hadron interactions.
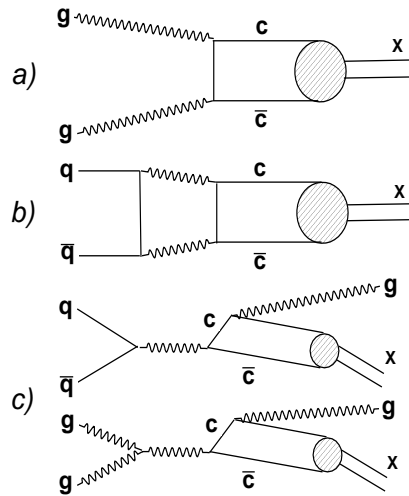

Fig. 9. Lowest-order parton fusion diagrams for hadronic χ production: a) gluon fusion, b) quark-antiquark annihilation, c) color evaporation.

The hadronic production of the χ states involves three parton fusion diagrams (**Fig. 9**): gluon fusion, light quark annihilation and color evaporation. However, the

relative contributions of each subprocess and even the total cross-section for charmonium production have proven difficult to calculate reliably. There are fairly definite predictions for the relative production rates of the χ states which may help distinguish among the models. The theoretical predictions for the ratios $\sigma(\chi_1)/\sigma(\chi_2) = \sigma(\chi(3510))/\sigma(\chi(3555))$ are as follows [21]: zero for gluon fusion, 4.0 for light quark fusion and 0.6 for color evaporation.

In this experiment the separation of χ_1 (3510 MeV) and χ_2 (3555 MeV) is possible. The matrix element for χ_1 production via gluon fusion is calculated to be zero according to the lowest-order QCD [22]. χ_1 can not be produced via gluon fusion because two spin-1 particle can not contribute to spin-1 particle production. If few χ_1 events are detected, then gluon fusion is dominant in χ_2 production.

Measurement of the χ_2 production asymmetry via gluon-gluon fusion is a cleanest way to define gluon contribution:

$$A_{LL}(x_F) = \hat{A}_{LL} \cdot \Delta G/G(x_1) \cdot \Delta G/G(x_2) \tag{6}$$

where x_1, x_2 -part of proton momentum, carried out by gluons ($M^2(\chi_2) = x_1 \cdot x_2 \cdot S$), x_F - Feynman variable of χ_2 -state, $\hat{A}_{LL}$– asymmetry on parton level for two fully polarized gluons ($\hat{A}_{LL} = -1$ in the model of gluon-gluon fusion). If the number of χ_1 events is significant, we need also to include other processes in the calculations to determine $\Delta G/G$. Note that $A_{LL}(p_\uparrow + p_\uparrow \to \chi_1 + X)$ and the $\chi_1 \to J/\Psi + \gamma$ decay angular distribution will be measured simultaneously in this case, providing an additional input for understanding the production process and the value of $\Delta G/G$ near $x = 0.3$. Last result of COMPASS experiment indicates that this region is extremely important [23], because $\Delta G/G$ has a maximum exactly at $x = 0.3$ in one solution (**Fig. 10**).

If all three charmonium production processes contribute, the measurement of χ_2, χ_1, and J/Ψ become equally important. The A_{LL} (χ_2, χ_1, J/Ψ) provide a test to various models, which predict opposite A_{LL} signs. The signs and magnitudes of the asymmetries will provide crucial information on the production mechanism(s), if the χ_1 production at 70 GeV in pp-interactions is not negligible compare to the χ_2 production.

Fig. 10. The solution of $\Delta G/G$ from experiment COMPASS. Figure from [23].

The study of χ_c states was carried out by Goliath and E-771 experiments. Registration of the γ-quanta from J/Ψ decay using it's conversion to e^+e^- pair allowed to distinguish between χ_c states (**Fig. 11**), but significantly decreased the efficiency and statistics. Pure statistics did not allow to measure the cross-section ratio $\sigma(\chi_1)/\sigma(\chi_2)$ with good accuracy. The error of the world average value (0.31 ± 0.14) is too high to define charmonium production mechanism (**Fig. 12**).
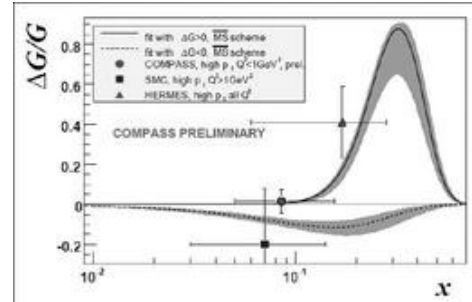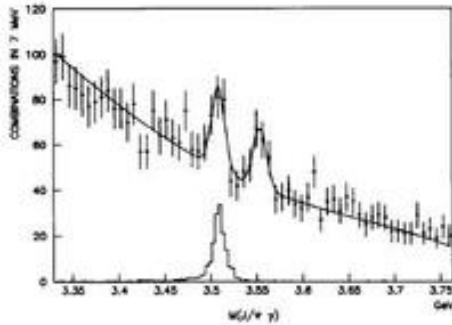
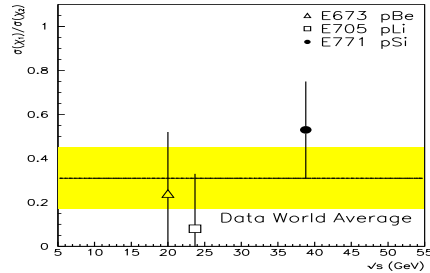Fig. 11. $J/\Psi + \gamma$-mass spectra from the Goliath experiment

Fig. 12. World data on $\sigma(\chi_1)/\sigma(\chi_2)$ ratio

J/Ψ production at 40 GeV was studied in $\pi^- Cu$ interactions [24]. Total J/Ψ production cross-section at $x_F > 0$ is (980 ± 120) nb for Cu nucleus or ≈ 15 nb per nucleon. Total J/Ψ production cross-section in pp-interaction at 40 GeV is about 2 nb per nucleon, but energy dependence of the cross-section is significant due to the increase of the gluon fusion contribution with energy. The expected value of the J/Ψ production cross-section in pp-interaction at 70 GeV is 15 nb.

3.2.1 MC-simulation

The main experimental challenge is to separate two close narrow states — χ_1 (3510 MeV) and χ_2 (3555 MeV). Mass resolution must be better, than their 1 % mass difference. In order to study the requirements for the experimental equipment and to estimate the expected statistics MC-simulation of the processes was carried out at following conditions:

- PYTHIA was used as a standard generator.
- Only gluon-gluon fusion and color evaporation diagrams for the χ_c production were used for reconstruction study (including quark-antiquark annihilation diagram does not change mass spectra).
- χ_c - states ($\chi_0(3410), \chi_1(3510)$ and $\chi_2(3555)$) decays to $J/\Psi + \gamma$ were studied.
- J/Ψ-decay was studied only in muon mode.
- MC was carried out for several values of the charge particle's momentum resolution and for the two values of the energy resolution of an electromagnetic calorimeter (ECal). The accuracy of the primary vertex reconstruction in beam direction is $\sigma_z = 10$ mm.
- The value of charge particle track momentum resolution is presented for 10 GeV particle.
- The influence of kinematic 1C-fit for J/Ψ (J/Psi- mass is fixed, 3-momentum components are fitted) to χ_c states mass resolution and the improvement of the separation was studied.

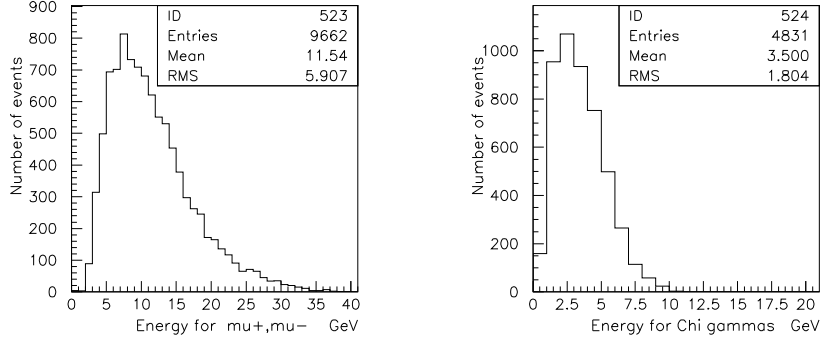Fig. 13. Energy distribution of $\mu^+(\mu^-)$ from J/Ψ-decay (left) and γ-quanta from χ_c-decays.

Average energy of $\mu^+(\mu^-)$-mesons registered from J/Ψ decay is 11.5 GeV and average energy of registered γ-quanta from χ_c-decay is 3.5 GeV (**Fig. 13**). According to the decay kinematics of χ_2, the γ's are effectively detected at very forward angle (up to 150 mrad). A calorimeter for detection of these γ's must have good energy resolution. χ_c states can not be disentangled by lead-glass electromagnetic calorimeter with the resolution $\sigma(E)/E = 12.5\,\%/\sqrt{E}$ (see **Fig. 14**) even with perfect momentum resolution $\delta p/p = 0.3\,\%$. The distribution does not change when introducing $1C$ fit on J/Ψ-mass.
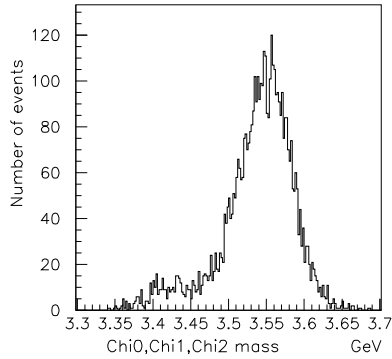

Fig. 14. Reconstruction of χ_c-mass **without** $1C$ fit. Track momentum resolution $\delta p/p = 0.3\%$. EMC energy resolution $\sigma(E)/E = 12\%/\sqrt{E}$.
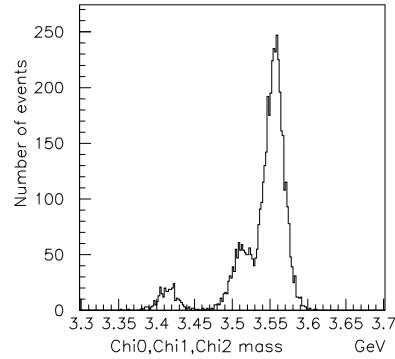
Fig. 15. Reconstruction of χ_c-mass **without** $1C$ fit. Track momentum resolution $\delta p/p = 0.4\%$. EMC energy resolution $\sigma(E)/E = 2.5\%/\sqrt{E}$.

χ_c peaks are clearly seen when using the calorimeter with resolution $\sigma(E)/E = 2.5\,\%/\sqrt{E}$ (see **Fig. 15**) even with slightly worse momentum resolution $\delta p/p = 0.4\,\%$ and without $1C$ fit procedure on J/Ψ-mass. Introducing $1C$ fit procedure on

J/Ψ-mass improves the distribution (**Fig. 16**). The mass spectra with generated charge particle momenta is also presented on **Fig. 17**.
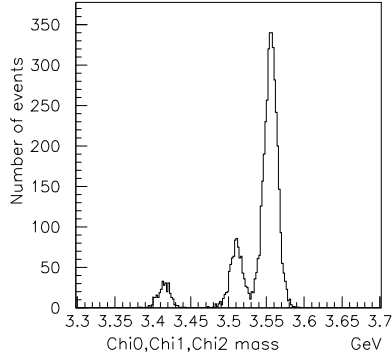

Fig. 16. Reconstruction of χ_c-mass **with** the use of $1C$ fit on J/Ψ-mass. $\delta p/p = 0.4\,\%$. $\sigma(E)/E = 2.5\,\%/\sqrt{E}$.
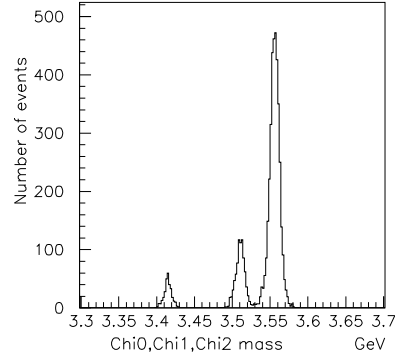
Fig. 17. Reconstruction of χ_c-mass with $\mu^+(\mu^-)$ momentum from PYTHIA. $\sigma(E)/E = 2.5\%/\sqrt{E}$.

3.2.2 Experimental Setup

MC study proved the possibility to separate χ_c-states and provided following requirements for the experimental setup:

- Possibility to work with $5 \cdot 10^6$ interactions per cycle (3 sec table, duty factor $1/3$, beam intensity $5 \cdot 10^7$ p/cycle).

- Large acceptance for Charmonium and Drell–Yan processes detection;

- EMC energy resolution $\sigma(E)/E = 2.5\,\%/\sqrt{E}$ at least at the central region, required for χ_c separation.

- Charge particle momentum resolution $\delta p/p = 0.4\,\%$ at $10\,\mathrm{GeV}$.

- Good separation of electrons and muons from hadrons, (charm production is at the level of 10^{-7}–10^{-8} per interaction in the target).

- Very fast DAQ to write information with the rate up to $100\,\mathrm{Mb/sec}$ (to study different inclusive processes with large cross-section).

The proposed schema of the experimental setup (**Fig. 18**) consists of seven different systems.

Fast scintillation counters and fiber hodoscopes will be used for beam trigger and coordinate reconstruction. Such type of fiber hodoscopes with the diameter of 0.28 mm was developed for DIRAC experiment. Light response is 10–12 photoelectrons for each fiber.
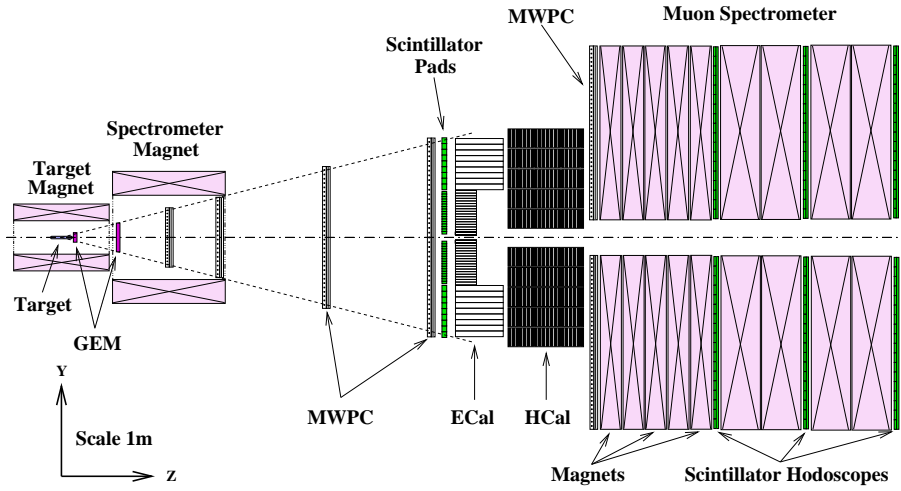
Fig. 18. SpAsCharm Experimental Setup

Transversely and longitudinally polarized targets are required for double-spin asymmetry measurements. The best solution is NH_3 target with the best figure of merit for polarized hydrogen targets.

Magnet spectrometer will consist of the magnet with the aperture 1.2 (horizontal) $\times 1$ (vertical) $\times 1\,m^3$ and field 15 kGs. Two or even three triple-GEM detectors with coordinate resolution better than 70 microns (or similar) will be used as the tracking detectors before the magnet. Three stations of MWPC or mDC will be used for the tracking detectors after spectrometer magnet. Such schema allows to obtain momentum resolution better than $\delta p/p = 0.04 \cdot P \cdot 10^{-2}\,c/GeV$ without taking into account multiple scattering.

Electromagnetic calorimeter for γ-quanta registration will consist of two parts. The central part (Θ_{lab} from 10 mrad to 125 mrad) of the calorimeter system consists of 1216 blocks of lead tungstate ($2.8 \times 2.8 \times 22\,cm^3$ per each block) to ensure good energy resolution of the γ detection. This is an array of 35×35 blocks with a hole of 3×3 blocks in the center for non-interacted beam. The properties of lead tungstate (PWO) calorimeters have been extensively studied at IHEP over last several years [25]. The energy resolution of 2 % at $E = 1\,GeV$ has been measured. The 2028 lead-glass or lead-scintillator counters ($3.81 \times 3.81 \times 45\,cm^3$ per each block) cover a large area (Θ_{lab} from 125 mrad to 250 mrad) and will be used mainly for separation of electrons and hadrons together with tracking system and hadron calorimeter. This is an array of 52×52 blocks with a hole of 26×26 in the center to accept the lead tungstate blocks.

The scintillator-pad trigger hodoscope containing 100 pads segmented mosaic structure before ECal will be used for the trigger.

Compensated lead-scintillator hadron calorimeter [26] will be assembled from $10 \times 10\,cm^2$ modules (6.5 nuclear length).

A muon detector will be upgraded on base of existing muon spectrometer of JINR-IHEP neutrino detector. The block of proportional chambers will be installed before muon detector to coincide muon tracks with charged ones in tracking system.

3.2.3   Efficiency and expected accuracy

The geometry of the experimental setup was chosen to achieve the maximal efficiency in J/Ψ and χ_c registration. Geometry acceptance is 61 % for J/Ψ registration in lepton decay mode and Drell–Yan and 31 % for χ_c-states (**Fig. 19**). Kinematic x_F region of detected χ_2 is presented on **Fig. 20**. The conservative estimation of J/Ψ event rate was done at following conditions:

- existing polarized propane-diol 20 cm long target;

- geometrical acceptance is 60 %;

- trigger, reconstruction and accelerator efficiencies are 0.9, 0.6 and 0.8 correspondingly.

- beam intensity is $5 \cdot 10^6$ π^-/cycle at 40 GeV and $5 \cdot 10^7$ p/cycle at 70 GeV.
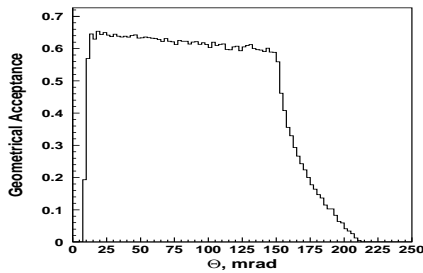
- J/Ψ registration in two lepton modes.

Fig. 19. Geometrical Acceptance for χ_2 at $x_F > 0$, γ-quanta is detected in PWO ($10 < \Theta < 125$ mrad, $\mu^+(e^+)$ and $\mu^-(e-)$) from J/Ψ decay are detected in the angle range $10 < \Theta < 250$
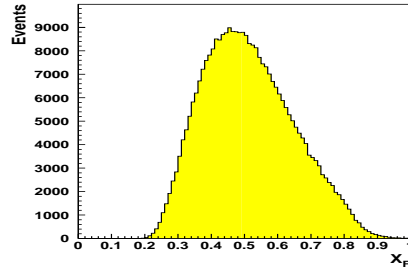
Fig. 20. Kinematic x_F region of detected χ_2 state

J/Ψ will be produced with the probability $2.42 \cdot 10^{-9}$ for incident particle or 4–5 events per hour. The integral number of registered J/Ψ is 4000 for pion beam for 40–day of statistics data taking. Single spin A_N statistic error is 14 %. The number of J/Ψ registered in pp-interactions is ten times larger for the same time. The accuracy of single-spin asymmetry is 4.5 % for J/Ψ and 12–20 % for χ_1/χ_2-states. The statistics may be increased by factor of two by using NH_3 target and by additional factor of two increasing extracted beam intensity.

Statistics may be increased for J/Ψ as well as for χ_1/χ_2-states studying J/Ψ production also in hadron modes. Geometrical efficiency (with branching) for two lepton modes is 7.2 %, for three hadron modes 2.5 %. We conservatively estimated

ECal energy resolution $\sigma(E)/E = 8\%/\sqrt{E}$ for hadron modes, assuming that at least one gamma from π^0-decay is outside Ecal central region.

3.2.4 Experiment schedule

Two main stages of the experiment are devoted to different main tasks. Stage 1 (with "old" polarized target and without polarized beam) is devoted to single-spin asymmetry measurements of J/ψ and χ_c inclusive production using pion and unpolarized proton beam. The cross-section ratio for χ_1/χ_2 production will be measured to determine the mechanism of charmonium production.

The main goal of stage 2 (with longitudinally polarized beam and target) is to measure double-spin asymmetry A_{LL} in charmonium production to study $\Delta G/G(x)$. Also A_{NN} will be measured for Drell–Yan pairs to study transversity $h(x)$. Simultaneously A_{NN} and A_N in J/Ψ, χ_c production will be studied. SPASCHARM experimental setup is universal and will be used to study charmonium production using heavy ion beam.

SPASCHARM construction time is 6 years (beginning 2007), but we are discussing the possibility to start spin studies at 2010 before the all experimental sub-systems will be ready. The possible physics is a polarization study of light and strange resonances in inclusive and/or exclusive reactions. Particle identification is required for this stage. Existing calorimeters, magnet. muon detector and cherenkov counters may be used after small modernization. New tracking system (MWPC or mDC chambers, GEM detectors or similar) and new fast electronics and DAQ required.

4 Conclusion

The investigation of spin properties of the matter and namely hadron spin structure and the role of the spin in hadron reactions is studied at Protvino. Unexpected large spin asymmetry in neutral meson inclusive production have stimulated many theoretical models.

Precision measurements using a polarized proton beam are required to distinguish between the models. The acceleration of the polarized proton beam at U-70 accelerator will give us the possibility to investigate nucleon spin structure. Proposal of new experiment to measure double-spin asymmetry in charm production is a cleanest way to study gluon contribution to nucleon spin. Spin effects in many other reactions will be measured simultaneously. The proposed experiment will be complementary to existing experiments.

References

[1] V. L. Solovianov: in *Proc. of the 6th International Symposium on High-energy Spin Physics*, Protvino, Russia, 22–27 Sep 1986, Serpukhov, vol. 1, p.26.

[2] N. S. Amaglobeli et al.: Sov. J. Nucl. Phys. **50** (1989) 432, [Yad. Fiz. **50** (1989) 695].

[3] V. D. Apokin et al.: Preprint IHEP 97-38; Instrum. Exp. Tech. **41** (1998) 464.

[4] A. A. Asseev et al.: Nucl. Instr. Meth. **A330** (1993) 39.

[5] A. P. Bugorski et al.:Instrum. Exp. Tech. **44** (2001) 1.

[6] N. S. Borisov et al.:JINR Preprint 1-80-98, Dubna, 1980.

[7] G. A. Akopdjanov et al. Nucl. Instr. Meth **40** (1977) 441;
F. Binon et al. Nucl. Instr. Meth **188** (1981) 507.

[8] V. D. Apokin et al.: Phys. Lett. **B243** (1990) 461.

[9] A. N. Vasilev et al.: Phys. Atom. Nucl. **67** (2004) 1487, [Yad. Phys. **67** (2004) 1512.

[10] S. M. Troshin, N. E. Tyurin: IHEP Preprint (in Russian) 88-201 (1988).

[11] M. G. Ryskin: *Sov. J. Nucl. Phys.* **48** (1988) 708.

[12] A. N. Vasilev et al.: Phys. Atom. Nucl. **68** (2005) 1790, [Yad. Phys. **68** (2005) 1852.

[13] A. N. Vasilev et al.: Phys. Atom. Nucl. **67** (2004) 1495, [Yad. Phys. **67** (2004) 1520.

[14] A. N. Vasilev and V. V. Mochalov: Phys. Atom. Nucl. **67** (2004) 2169,
Yad. Phys. **67** (2004) 2193.

[15] V. V. Mochalov, S. M. Troshin and A. N. Vasiliev: Phys. Rev. **D69** (2004) 077503.

[16] A. S. Belov et al.: in *Proc. High energy spin physics, SPIN-1998* (1998) 622;
A. S. Belov, L. P. Netchaeva and A. V. Turbabin: Rev. Sci. Instrum. **77** (2006) 03A522.

[17] Ya. Derbenev, A. Kondratenko: Part. Acc. **8** (1978) 115.

[18] V. Ptitsyn, Yu. Shatunov: Nucl. Instr. Meth. **A398** (1997) 126.

[19] Ya. Derbenev et al.:*Proc. of 10-th Int. Conf. On High Energy Acc.* **v.2** (1977) 272.

[20] A. V. Batunin, S. R. Slabospitsky: Phys. Lett. **B188** (1987) 269;
Yad. Phys. **44** (1986) 1551.

[21] D. A. Bauer et al.: Phys. Rev. Lett. **54** (1985) 753.

[22] S. D. Ellis et al.: Phys. Rev. Lett. **36** (1976) 1263; C. E. Carlson and R. Suaya: Phys. Rev. **D14** (1976) 3115; C. E. Carlson and R. Suaya: Phys. Rev. **D18** (1978) 760;
R. Baier and R. Rucki: Phys. **C19** (1983) 251;
V. Barger and A. D. Martin: Phys. Rev. **D31** (1985) 1051.

[23] E. Santos: talk this conference.

[24] Yu. B. Bushnin et al.: Phys. Lett. **B72** (1977) 269.

[25] T. Brennan et al.: NIM **A494** (2002) 313; V. A. Batarin et al.: NIM **A510** (2003) 211; NIM **A510** (2003) 248; NIM **A512** (2003) 484; NIM **A534** (2004) 486;
NIM **A530** (2004) 286; NIM **A540** (2005) 131; NIM **A550** (2005) 543.

[26] G. A. Alekseev et al.: Nucl. Instr. Meth. **A461** (2001) 381.